



## Observation of Topological Phase Transitions in Photonic Quasicrystals

Mor Verbin,<sup>1</sup> Oded Zilberberg,<sup>2</sup> Yaacov E. Kraus,<sup>2</sup> Yoav Lahini,<sup>1,3</sup> and Yaron Silberberg<sup>1</sup>

<sup>1</sup>*Department of Physics of Complex Systems, Weizmann Institute of Science, Rehovot 76100, Israel*

<sup>2</sup>*Department of Condensed Matter Physics, Weizmann Institute of Science, Rehovot 76100, Israel*

<sup>3</sup>*Department of Physics, Massachusetts Institute of Technology, Cambridge, Massachusetts 02139, USA*

(Received 26 November 2012; published 14 February 2013)

Topological insulators and topological superconductors are distinguished by their bulk phase transitions and gapless states at a sharp boundary with the vacuum. Quasicrystals have recently been found to be topologically nontrivial. In quasicrystals, the bulk phase transitions occur in the same manner as standard topological materials, but their boundary phenomena are more subtle. In this Letter we directly observe bulk phase transitions, using photonic quasicrystals, by constructing a smooth boundary between topologically distinct one-dimensional quasicrystals. Moreover, we use the same method to experimentally confirm the topological equivalence between the Harper and Fibonacci quasicrystals.

DOI: [10.1103/PhysRevLett.110.076403](https://doi.org/10.1103/PhysRevLett.110.076403)

PACS numbers: 71.23.Ft, 05.30.Rt, 73.43.Nq

The classification of gapped systems, such as band insulators and superconductors, by topological indices is a rapidly developing paradigm in condensed matter physics [1]. This novel approach provides insights into the characterization of states of matter, as well as predicts exotic phenomena.

The topological classification of a system assigns an integer index to its energy gap. This index encodes properties that are robust to distortions and deformation of the system. Hence, when a system with a given index is continuously deformed into a system whose index has a different value, the bulk energy gap must close, namely a quantum phase transition occurs. Accordingly, if a system can be continuously deformed into another system while keeping the bulk gap open, then their topological indices must be the same, defining them as topologically equivalent. Usually, such a phase transition manifests by the appearance of gap-traversing states at a sharp boundary between a topologically nontrivial material and the topologically trivial vacuum. Examples for such boundary states are the chiral modes of the integer quantum Hall effect (IQHE), the Dirac cone of the three-dimensional topological insulator, and the Majorana fermions of one-dimensional (1D) topological superconductors [1].

A new type of topological phenomena has been recently studied in quasiperiodic systems [2,3]. Such systems, which are ordered but not periodic, were shown to be characterized by topological indices that are usually attributed to systems of a dimension higher than their physical dimension. In particular, it was shown that the canonical 1D quasiperiodic systems, i.e., the Harper (or Aubry-André) model [4,5], the diagonal Fibonacci model [6], and their quasicrystalline off-diagonal variants [7,8], can be assigned Chern numbers. These numbers are topological indices that characterize generic two-dimensional (2D) systems. A continuous deformation between two quasicrystals (QCs) with different Chern numbers will therefore

result in a bulk phase transition. Correspondingly, at a sharp boundary between such a QC and the vacuum, localized subgap boundary states may appear. These states were experimentally observed in photonic Harper QCs [2]. Further analyses of 1D topological QCs with sharp boundaries have been conducted in cold atoms [9] and superconducting wires [10].

In systems where the topology is generated by a symmetry which is broken at the boundary, the boundary phenomenon is not robust [11,12]. Similarly, the topological characterization of a QC is based on its long-range order, which is broken at the sharp boundary. Therefore, its boundary states do not always appear. However, if the boundary between a topologically nontrivial QC and a topologically trivial system is adiabatically smooth, subgap states will always appear at the boundary, revealing the bulk gap closure. Accordingly, a smooth boundary can be used to prove equivalence between different quasiperiodic systems, if the energy gap remains open throughout the deformation.

In this Letter, we study the bulk gap closure that occurs when smoothly deforming between topologically inequivalent quasiperiodic systems, and its absence when the systems are topologically equivalent. To this end, we create two inequivalent Harper QCs, and spatially deform between them. We then observe the closure of bulk energy gaps through the emergence of subgap states localized within the deformation region. In contrast, using the same interpolation process between seemingly different but topologically equivalent systems, the Harper and the Fibonacci QCs, no such phase transition is observed, thereby confirming that these two models are indeed topologically equivalent. These phenomena are experimentally tested in quasiperiodic photonic lattices, where the phase transition, or its absence, is directly observed using the propagation of light in waveguide arrays.

Photonic lattices are widely used for realizations of different models originating from solid state physics,

due to the high level of control over their parameters and behavior [13]. Our photonic QCs are composed of an array of coupled single-mode waveguides, fabricated in bulk glass using femtosecond laser microfabrication technology [14]. The overlap between the evanescent modes of the waveguides allows the propagating light to tunnel from each waveguide to its neighboring waveguides. Hence, the hopping amplitude between adjacent waveguides can be controlled by modulating the spacing between them.

The dynamics of light propagating in these coupled waveguide arrays is described by the tight-binding model, with the propagation axis  $z$  taking over the role of time,  $i\partial_z \psi_n = H\psi_n$ , where  $\psi_n$  is the wave function at waveguide number  $n$ . Taking the hopping amplitude to be real, we obtain the general Hamiltonian

$$H\psi_n = t_n\psi_{n-1} + t_{n+1}\psi_{n+1}, \quad (1)$$

where  $t_n$  is the hopping amplitude from site  $n$  to site  $n - 1$ .

Our intention is to study the transition that occurs when some system I is deformed into another system II, where each system has its own set of quasiperiodic hopping amplitudes  $t_n^I$  and  $t_n^{II}$ , respectively. To this end, we fabricate a waveguide array with a deformed hopping profile  $t_n = f_n t_n^I + (1 - f_n)t_n^{II}$ , where

$$f_n = \begin{cases} 1 & 1 \leq n \leq L_I \\ 1 - \frac{n-L_I}{L_D} & L_I < n < L_I + L_D \\ 0 & L_I + L_D \leq n \leq L_I + L_D + L_{II} \end{cases}, \quad (2)$$

as depicted in Fig. 1(a). This procedure produces an array of length  $L_I$  of system I on one side of the structure, an array of length  $L_{II}$  of system II on the other side, and an  $L_D$ -long deformation region, which continuously transforms between the two. This structure enables the study of the eigenstates of both systems as well as the transition between them, on a single waveguide array.

The properties of the Hamiltonian fabricated within the photonic crystal are studied by injecting light into one of the waveguides in the array and measuring the outgoing intensity at the output facet using a CCD camera, as illustrated in Fig. 1(b). The injected beam excites a wave packet of all the modes that have a nonvanishing amplitude at the injection site, and the light propagates in the lattice according to this superposition of eigenstates. The width of the outgoing intensity distribution can therefore reveal the existence of localized eigenstates: If there is no localized state near the injection site, the light spreads freely throughout the array, propagating according to the bulk properties of the system. However, when light is injected in the vicinity of a localized state, its expansion is dominated by the width of the state. To quantify the localization of the outgoing light, we measure the amount of light that remains within a small

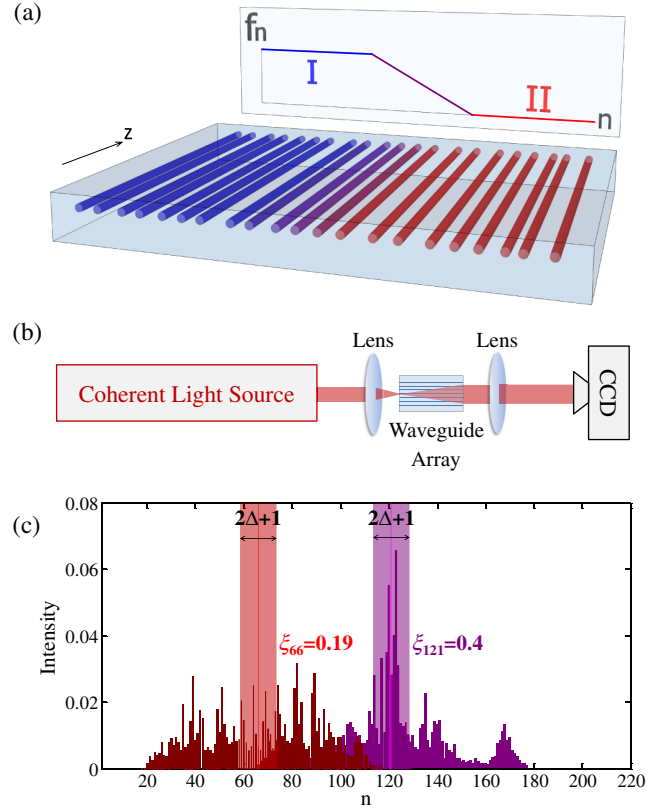


FIG. 1 (color online). Experimental methods. (a) Illustration of a photonic waveguide array implementing a deformation between two QCs [cf. Eq. (2)]. (b) A schematic of the experimental setup. We focus a coherent light beam into a waveguide in the array, allow it to propagate along the structure, and image the output intensity using a CCD camera. (c) Illustration of the relation between the localization parameter  $\xi_n$  and the measured intensity distribution  $|\psi_n|^2$  for two injection sites,  $n = 66$  and  $n = 121$ . The shaded intervals denote the  $\Delta$ -distance neighborhood around the insertion point. When more light remains within this neighborhood, the value of  $\xi_n$  increases.

distance  $\Delta$  from the injection site  $n$ , by measuring the generalized return probability [15],

$$\xi_n = \left( \sum_{m=n-\Delta}^{n+\Delta} |\psi_m|^2 \right) / \left( \sum_{m=1}^{L_I+L_D+L_{II}} |\psi_m|^2 \right). \quad (3)$$

The relation between  $\xi_n$  and the intensity distribution  $|\psi_n|^2$  is illustrated in Fig. 1(c). Since  $\xi_n$  is meant to reveal the existence of localized states, we will choose  $\Delta$  to be of the order of the width of a localized subgap state.

Let us now introduce the specific quasiperiodic tight-binding models under study. In these models the hopping amplitude is modulated according to

$$t_n = t_0[1 + \lambda d_n], \quad (4)$$

where  $t_0$  is the characteristic hopping amplitude of the system,  $\lambda \in [0, 1)$  is the modulation strength, and  $d_n \in [-1, 1]$  is some quasiperiodic modulation function.

Here we consider two such modulations: the Harper modulation

$$d_n^H = \cos(2\pi bn + \phi), \quad (5)$$

and the Fibonacci-like modulation

$$d_n^F = 2 \left( \left\lfloor \frac{\tau}{\tau+1}(n+2) \right\rfloor - \left\lfloor \frac{\tau}{\tau+1}(n+1) \right\rfloor \right) - 1 = \pm 1. \quad (6)$$

The long-range order of the Harper QC [7] is controlled by the modulation frequency  $b$ . Whenever  $b$  is irrational, the hopping modulation is incommensurate with the underlying lattice, resulting in a quasiperiodic pattern. Accordingly, the parameter  $\phi$  shifts the origin of the modulation. Comparably, the Fibonacci-like QC is constructed from a sequence of two values that are ordered in a quasiperiodic manner. This sequence is obtained by applying the “cut-and-project” procedure on a square lattice onto the line  $y = x/\tau$  [16]. Whenever the slope of the line,  $\tau$ , is irrational, the sequence is quasiperiodic. For example, the case of  $\tau = (1 + \sqrt{5})/2$  is the well-known Fibonacci QC.

The energy spectrum of the Harper QC is composed of a fractal set of bands and gaps, in a way that depends on the modulation frequency  $b$  [7,17]. These gaps are associated with Chern numbers, which are also uniquely determined by  $b$  [3]. For any rational approximant  $b = p/q$ , the Chern number  $\nu_r$  that is associated with a gap number  $r = 1, \dots, (q-1)$  abides the Diophantine equation  $r = \nu_r q + t_r p$ , where  $\nu_r$  and  $t_r$  are integers, and  $0 < |\nu_r| < q/2$  [18]. The distribution of Chern numbers for an irrational  $b$  is given by taking the appropriate limit of  $p$ ,  $q \rightarrow \infty$ . Hence, the gaps of two Harper QCs with  $b_I \neq b_{II}$  are associated with different distributions of Chern numbers. Thus, when deforming between two such models the Chern number distribution rearranges by level crossings. This makes these models topologically inequivalent.

The properties of the Fibonacci-like QC differ in many ways from those of the Harper QC, e.g., the localization of the bulk wave functions [6–8,19]. Nevertheless, it was recently shown that they are topologically equivalent whenever the frequency of the Harper modulation satisfies  $b = (\tau + 1)/\tau$  [3]. In such a case, the gaps of the Fibonacci-like QC are associated with the same Chern numbers as those of the Harper QC. Hence, for a given modulation frequency  $b$ , the Harper QC can be continuously deformed into the Fibonacci-like QC without the appearance of a phase transition.

Note that the deformation in Eq. (5) contains an addition degree of freedom in the form of the parameter  $\phi$ . This parameter has a crucial role in the observation of the topological boundary states of quasiperiodic systems [2]. While the spectrum of our model is gapped in the bulk, localized boundary states appear, which traverse the energy gaps as a function of  $\phi$ . Nevertheless, in this Letter we focus on bulk properties, which are  $\phi$  independent [20].

We now turn to our experimental results. We construct a deformation between topologically inequivalent Harper QCs with modulation frequencies  $b_I \neq b_{II}$ . Figure 2(a) depicts the hopping amplitudes of a deformation between a Harper QC with  $b_I = 2/(1 + \sqrt{5})$  and a Harper QC with  $b_{II} = 2/(1 + \sqrt{6.5})$ , where  $t_0 = 28/75 \text{ mm}^{-1}$ ,  $\lambda = 0.475$ , and  $\phi_I = \phi_{II} = \pi$ . For this set of parameters, the bulk wave functions of the Harper QCs are extended [7]. We fabricated this structure in a 75 mm-long photonic waveguide array. This results in an effective propagation of 14 tunneling lengths, where the tunneling length is the characteristic length for hopping, namely  $2/t_0$ . With such a propagation length, light injected in the bulk of the structure will sufficiently expand in comparison to the width of localized subgap states.

To experimentally observe the phase transition between the two QCs, a 808 nm continuous-wave diode laser beam was injected into each waveguide with a  $\times 40$  microscope objective. The light at the output facet was imaged onto a CCD camera using a  $\times 5$  microscope objective. Using the measured light distribution, we obtained  $\xi_n$  as a function of the injection site  $n$ . The results are presented in Fig. 2(b). Two clear peaks in the deformation region can be seen over a relatively flat  $\xi_n$  outside the region. This is a clear indication of the existence of localized states within the deformation region. Note that measurements of  $\xi_n$  for  $n < 30$  and  $n > 190$  are omitted from this plot—for these injection sites the expanding light hits the edges of the structure, causing  $\xi_n$  to be skewed by boundary effects.

To reveal the source of the peaks observed in  $\xi_n$ , we numerically obtain the local density of states (LDOS), which is presented in Fig. 2(c). The LDOS is defined by  $D_n(E) = \sum_m \delta(E - E_m) |\varphi_n^{(m)}|^2$ , where  $E_m$  is the energy of the  $m$ th eigenstates, and  $\varphi_n^{(m)}$  is its wave function.  $D_n(E)$  describes the spatial distribution of the eigenstates of the structure as a function of energy. For  $n \leq L_I$ , we observe bands of extended states that correspond to the eigenstates of system I. Similarly, for  $n \geq L_I + L_D$  we recognize the band of extended states of system II. However, along the deformation region, there are few spatially localized states with energies that discretely traverse the gaps. These subgap states are the origin of the measured peaks in  $\xi_n$ . Their appearance is an explicit signature of the phase transition between the inequivalent QCs since they traverse the gap continuously when  $L_D \rightarrow \infty$  [20]. We have therefore experimentally observed the bulk phase transition between two topologically inequivalent Harper QCs.

We now turn to study the transition between topologically equivalent QCs. We constructed a deformation between a Harper QC and Fibonacci QC, with a matched modulation frequency  $b_I = (\tau_{II} + 1)/\tau_{II} = 2/(1 + \sqrt{5})$  [21]. The hopping amplitudes  $t_n$  are depicted in Fig. 2(d), for  $t_0 = 28/75 \text{ mm}^{-1}$ ,  $\lambda = 0.225$ , and  $\phi = \pi(1 + 3b)$ . For this set of parameters, the bulk wave functions of the Harper QC are extended, while those of the Fibonacci

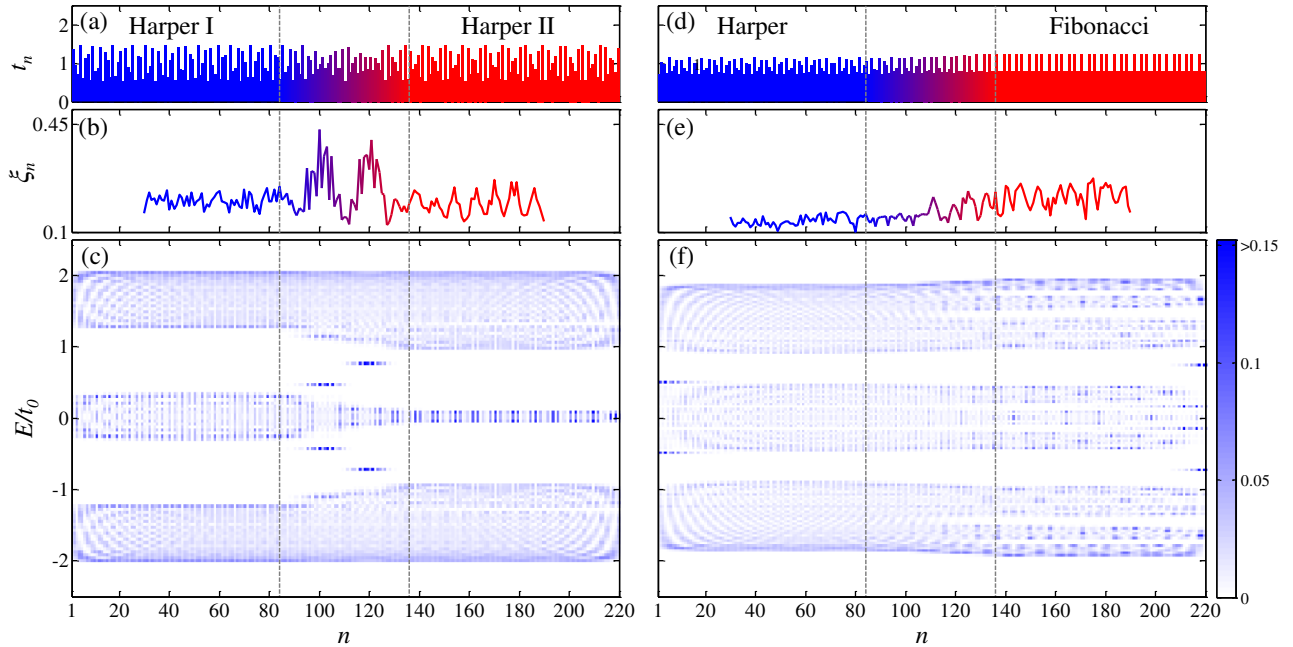


FIG. 2 (color online). Summary of results for a smooth deformation between (a)–(c) two topologically inequivalent Harper QCs, and (d)–(f) topologically equivalent Harper and Fibonacci QCs. In both experiments (from left to right),  $L_I = 84$  (blue),  $L_D = 51$  (purple hues), and  $L_{II} = 84$  (red). (a) The hopping amplitude  $t_n$  as a function of the lattice site  $n$ , for modulation frequencies  $b_I = 2/(1 + \sqrt{5})$  and  $b_{II} = 2/(1 + \sqrt{6.5})$  of the Harper QCs. (b) Experimentally measured  $\xi_n$  for  $\Delta = 7$ , as a function of the injection site  $n$ . The two peaks within the deformation region imply the existence of localized states. (c) Numerically obtained LDOS of the structure,  $D_n(E)$ . The energy bands are composed of extended states, while localized states (roughly 15 sites wide) traverse the gaps in the deformation region. These states manifest the transition between the inequivalent QCs. (d)–(f) Same as (a)–(c), but with a Harper QC deformed into a Fibonacci QC with  $b_I = (\tau_{II} + 1)/\tau_{II} = 2/(1 + \sqrt{5})$ . Here,  $\xi_n$  shows no sign of localized states. Accordingly, though the distribution of the bands changes along the structure, the energy gaps appear to remain open. This confirms the equivalence between the two QCs.

are critical [8]. Nevertheless, for the structure's effective propagation length, light injected into the bulk of both QCs will sufficiently expand in comparison to the width of potential localized states. The measured  $\xi_n$  of this system is depicted in Fig. 2(e), showing no sign of localized states within the deformation region. The numerically obtained LDOS is shown in Fig. 2(f). While the configuration of the bands changes considerably between the two QCs, no gap closure is observed along the deformation. Note, also, that two subgap states appear at the sharp boundaries with the vacuum [20]. The open gaps and the corresponding absence of peaks in  $\xi_n$  serve as experimental confirmation of the equivalence between the Fibonacci and the Harper QCs.

To conclude, in this Letter we have presented a novel method to study topological phase transitions using a continuous deformation between two systems, which acts as a smooth boundary between them. When the boundary is sufficiently smooth, observations of subgap states localized within the deformation area serve as evidence of the phase transition. Such subgap states do not appear when a phase transition does not take place, namely, between topologically equivalent systems. Our method extends the prevailing approach which focuses on states that appear at

sharp boundaries between topologically nontrivial systems and the vacuum. It has proven useful in studying the topological characterization of 1D quasiperiodic systems, since it circumvents the subtlety of their boundary phenomena at sharp boundaries. Furthermore, this technique may be useful to study other topological systems, such as (i) the weak and the crystalline topological insulators, where the surface breaks the underlying symmetry [11,12], (ii) varying dopant concentration in 3D topological insulators [22], and (iii) nanowires that may host Majorana fermions at their boundaries [23].

We thank Y. Avron, R. Lifshitz, A. Keselman, and S. Huber for fruitful discussions. We thank the U.S. Israel Binational Science Foundation, the Minerva Foundation of the DFG, Crown Photonics Center, ERC Advanced Grant Quami, and ISF Grant No. 700822030182 for financial support.

- 
- [1] M. Z. Hasan and C. L. Kane, *Rev. Mod. Phys.* **82**, 3045 (2010); X.-L. Qi and S.-C. Zhang, *ibid.* **83**, 1057 (2011).
  - [2] Y. E. Kraus, Y. Lahini, Z. Ringel, M. Verbin, and O. Zeitlinger, *Phys. Rev. Lett.* **109**, 106402 (2012).

- [3] Y.E. Kraus and O. Zeitlinger, *Phys. Rev. Lett.* **109**, 116404 (2012).
- [4] P.G. Harper, *Proc. Phys. Soc. London Sect. A* **68**, 874 (1955).
- [5] S. Aubry and G. André, *Ann. Isr. Phys. Soc.* **3**, 133 (1980).
- [6] M. Kohmoto, L. P. Kadanoff, and C. Tang, *Phys. Rev. Lett.* **50**, 1870 (1983); S. Ostlund, R. Pandit, D. Rand, H. J. Schellnhuber, and E. D. Siggia, *ibid.* **50**, 1873 (1983).
- [7] J. H. Han, D. J. Thouless, H. Hiramoto, and M. Kohmoto, *Phys. Rev. B* **50**, 11365 (1994).
- [8] M. Kohmoto, B. Sutherland, and C. Tang, *Phys. Rev. B* **35**, 1020 (1987).
- [9] F. Mei, S.-L. Zhu, Z.-M. Zhang, C.H. Oh, and N. Goldman, *Phys. Rev. A* **85**, 013638 (2012); L.-J. Lang, X. Cai, and S. Chen, *Phys. Rev. Lett.* **108**, 220401 (2012); Z. Xu, L. Li, and S. Chen, arXiv:1210.7696.
- [10] M. Tezuka and N. Kawakami, *Phys. Rev. B* **85**, 140508 (2012); O. Viyuela, A. Rivas, and M. A. Martin-Delgado, *Phys. Rev. B* **86**, 155140 (2012); W. DeGottardi, D. Sen, and S. Vishveshwara, arXiv:1208.0015; X. Cai, L.-J. Lang, S. Chen, and Y. Wang, arXiv:1208.2532; I. I. Satija and G. G. Naumis, arXiv:1210.5159.
- [11] Z. Ringel, Y.E. Kraus, and A. Stern, *Phys. Rev. B* **86**, 045102 (2012).
- [12] L. Fu, *Phys. Rev. Lett.* **106**, 106802 (2011); L. Fu and C. Kane, *Phys. Rev. Lett.* **109**, 246605 (2012).
- [13] F. Lederer, G. I. Stegeman, D. N. Christodoulides, G. Assanto, M. Segev, and Y. Silberberg, *Phys. Rep.* **463**, 1 (2008).
- [14] A. Szameit, D. Blömer, J. Burghoff, T. Schreiber, T. Pertsch, S. Nolte, A. Tünnermann, and F. Lederer, *Opt. Express* **13**, 10552 (2005).
- [15] Note that the case of  $\Delta = 0$  is the return probability,  $\xi_n = |\psi_n|^2$ . This generalization is required due to the finite width of subgap states.
- [16] M. Senechal, *Quasicrystals and Geometry* (Cambridge University Press, Cambridge, England, 1996).
- [17] D. R. Hofstadter, *Phys. Rev. B* **14**, 2239 (1976).
- [18] D. J. Thouless, M. Kohmoto, M. P. Nightingale, and M. den Nijs, *Phys. Rev. Lett.* **49**, 405 (1982).
- [19] S. Jitomirskaya and C. A. Marx, *J. Fixed Point Theory Appl.* **10**, 129 (2011).
- [20] See Supplemental Material at <http://link.aps.org/supplemental/10.1103/PhysRevLett.110.076403> for more details on the roles of  $\phi$  and  $L_D$ .
- [21] To align the energy spectra of the Harper and Fibonacci QCs, a constant shift is added to the hopping amplitude.
- [22] T. Sato, K. Segawa, K. Kosaka, S. Souma, K. Nakayama, K. Eto, T. Minami, Y. Ando, and T. Takahashi, *Nat. Phys.* **7**, 840 (2011).
- [23] V. Mourik, K. Zuo, S. M. Frolov, S. R. Plissard, E. P. A. M. Bakkers, and L. P. Kouwenhoven, *Science* **336**, 1003 (2012); G. Kells, D. Meidan, and P. W. Brouwer, *Phys. Rev. B* **86**, 100503(R) (2012); A. Das, Y. Ronen, Y. Most, Y. Oreg, M. Heiblum, and H. Shtrikman, *Nat. Phys.* **8**, 887 (2012).